# Perpendicular Magnetic Anisotropy Caused by Interfacial Hybridization via Enhanced Orbital Moment in Co/Pt Multilayers: Magnetic Circular X-Ray Dichroism Study

N. Nakajima,[1] T. Koide,[1] T. Shidara,[1] H. Miyauchi,[2] H. Fukutani,[2] A. Fujimori,[3] K. Iio,[4] T. Katayama,[5] M. Nývlt,[5] and Y. Suzuki[5]

[1]*Photon Factory, IMSS, High Energy Accelerator Research Organization, Tsukuba, Ibaraki 305, Japan*
[2]*Institute of Physics, University of Tsukuba, Tsukuba, Ibaraki 305, Japan*
[3]*Department of Physics, University of Tokyo, Bunkyou-ku, Tokyo 113, Japan*
[4]*Department of Physics, Tokyo Institute of Technology, Meguro-ku, Tokyo 152, Japan*
[5]*Electrotechnical Laboratory, Tsukuba, Ibaraki 305, Japan*

(Received 13 November 1997)

Magnetic circular x-ray dichroism (MCXD) measurements at the Co $L_{2,3}$ and $M_{2,3}$ core edges reveal a strongly enhanced perpendicular Co orbital moment ($m_{\mathrm{orb}}$) in Co/Pt multilayers which show perpendicular magnetic anisotropy (PMA). MCXD signals at the Pt $N_{6,7}$ and $O_{2,3}$ edges, arising from Pt $5d$-Co $3d$ hybridization, persist for the thinnest Co layer. The hybridization is shown to be localized at the Co/Pt interface and to cause the $m_{\mathrm{orb}}$ enhancement which drives PMA. Unambiguous evidence for a transition from fcc to hcp Co is presented and $m_{\mathrm{orb}}$ of bulk fcc Co has been determined to be $0.11\mu_B$ for the first time. [S0031-9007(98)07736-9]

PACS numbers: 75.70.Cn, 78.20.Ls, 78.70.Dm

Since the discovery of perpendicular magnetic anisotropy (PMA) in metallic overlayers and multilayers [1], this phenomenon has been a subject of great interest, particularly with regard to its microscopic origin. Despite numerous experimental and theoretical studies, a full understanding of PMA has not yet been achieved. Strong PMA appears for only a limited number of combinations of magnetic and nonmagnetic metals and for a particular crystal orientation, such as Co/Pd(111) and Co/Pt(111) [1,2]. First-principles calculations [3,4] predicted in-plane magnetic anisotropy for a free-standing Co monolayer, whereas they predicted PMA in free-standing Fe and V monolayers and some multilayers. These studies indicated the important role of nonmagnetic metals as well as the band structure in producing PMA. Experimental [5] and theoretical [6] studies have recently been reported that highlight the interfacial hybridization between magnetic and nonmagnetic metals concerning overlayer-induced anomalous PMA in ultrathin Co films. Since magnetic anisotropy is thought to originate mainly from the spin-orbit (SO) interaction, the orbital magnetic moment ($m_{\mathrm{orb}}$), which usually makes a small contribution to magnetism in $3d$ transition metals, was also expected to play an important role in PMA. A tight-binding approach to $m_{\mathrm{orb}}$ and magnetic anisotropy [7] indicated a close connection between these two quantities.

Magnetic circular x-ray dichroism (MCXD) in core-level absorption [8,9] allows an element-specific and separate determination of the orbital and spin moments in combination with the MCXD sum rules [10], thus providing a powerful technique for studying the magnetism of multicomponent systems, such as multilayers. An $m_{\mathrm{orb}}$ enhancement of Co and Fe was observed in Co/Pd, Co/Pt, and Fe/Pt multilayers by MCXD experiments [11,12]. Weller *et al.* [13] have recently shown by angle-dependent MCXD measurements that the $m_{\mathrm{orb}}$ anisotropy is the origin of PMA. Induced spin polarization in nonmagnetic metals was also observed in Co/Pt and Fe/Pd multilayers by MCXD measurements [14]. However, experimental evidence is still lacking for the relationship between $m_{\mathrm{orb}}$ and the interfacial hybridization regarding PMA.

In this Letter we present unambiguous evidence for a close connection between the enhanced perpendicular $m_{\mathrm{orb}}$ of Co and the Co $3d$-Pt $5d$ interfacial hybridization in Co/Pt multilayers. This is shown by MCXD measurements at *both* the Co $L_{2,3}$ and $M_{2,3}$ and the Pt $N_{6,7}$ and $O_{2,3}$ core edges on multilayers with systematically varying Co-layer thicknesses. We find that the $m_{\mathrm{orb}}$ enhancement and strong $3d$-$5d$ hybridization are highly localized at the Co/Pt interface, and show that these effects give rise to PMA. Furthermore, we present clear evidence of a structural transition from fcc to hcp Co with increasing Co-layer thickness and give $m_{\mathrm{orb}} = (0.110 \pm 0.01)\mu_{\mathrm{B}}/\mathrm{Co}$ for bulk fcc Co for the first time. This value is significantly smaller than that of bulk hcp Co [$(0.148 \pm 0.005)\mu_{\mathrm{B}}/\mathrm{Co}$], in good agreement with a recent theoretical prediction [15].

Ten Co($t_{\mathrm{Co}}$ ML)/Pt(7.5 ML) multilayer samples ($1.5 \leq t_{\mathrm{Co}} \leq 29$; ML = monolayer) with a total thickness of 850–1130 Å were prepared by rf sputtering in Kr onto water-cooled float-glass substrates. First, a 150-Å-thick Pt layer was grown and then annealed at 350 °C for 1 h, producing a fully fcc (111) textured buffer layer as confirmed by x-ray diffraction (XRD) analyses. Scanning tunneling microscopy observation revealed a 2500-Å average grain size and atomically flat terraces separated by monoatomic steps. The average terrace width was 50 Å. Then, the sequence of Co and Pt layers was grown by terminating with Pt as a protective layer. Low- and high-angle XRD analyses confirmed the superlattice period, which almost agreed

  

with the designed values. XRD satellite peaks are best reproduced by a model calculation which takes into account an intermixing of only 1 ML for each Co and Pt layer. The magnetic anisotropy of the samples was studied by torque magnetometry. PMA was found for $t_{\mathrm{Co}} \leq 5$ ML and in-plane anisotropy was seen for $t_{\mathrm{Co}} \geq 7$ ML. The samples were characterized by polar Kerr-hysteresis measurements in fields of up to 1.88 T. MCXD experiments were performed at room temperature using circularly polarized synchrotron radiation from helical undulators on BL-28A and AR-NE1B [16] at the Photon Factory. The photon helicity was fixed and the magnetic-field direction was switched parallel and antiparallel to it. From 40 to 100 eV, the MCXD in normal-incidence reflection was measured under a field of $\pm 2$ T using an ultrahigh-vacuum superconducting magnet [17]. Low-energy reflectivity was measured from 4 to 40 eV using BL-11C. The soft x-ray absorption (XAS) was measured by the total electron-yield method for the region, covering the Co $L_{2,3}$ core edges. A field of $\pm 1.1$ T was applied to the sample perpendicular to the film plane using a permanent-magnet MCXD apparatus for each photon energy.

Figure 1 shows the real part of the off-diagonal dielectric-tensor element ($\varepsilon^r_{xy}$) in the Co $M_{2,3}$ and Pt $N_{6,7}$ and $O_{2,3}$ edge regions, which was obtained from the reflection-MCXD and wide-range reflectivity spectra by the Kramers-Kronig analysis; $\varepsilon^r_{xy}$ represents the absorption MCXD spectrum. A correction for the degree of circular polarization ($P_{\mathrm{C}}$) was made using a measured average value of $P_{\mathrm{C}} = 92\%$ [18]. We display in the inset the imaginary part of the diagonal tensor element ($\varepsilon^i_{xx}$) for $t_{\mathrm{Co}} = 3$ and 15 ML, which stands for the normal absorption spectrum. Only a negative MCXD is observed at the Co $M_{2,3}$ edges for thin $t_{\mathrm{Co}}$, while a small positive MCXD is seen as well as a strong negative MCXD for thick $t_{\mathrm{Co}}$. The observed asymmetry increase of the MCXD spectrum shows an enhancement of $m_{\mathrm{orb}}$ of Co perpendicular to the film plane with decreasing $t_{\mathrm{Co}}$. A strong negative and a very weak positive MCXD are observed at the Pt $O_3$ and $O_2$ edges, respectively, for thin $t_{\mathrm{Co}}$. A positive and a negative MCXD are clearly seen at the Pt $N_7$ and $N_6$ edges, with the positive intensity being slightly stronger than the negative one. These observations show that magnetic moments are induced on Pt atoms by the strong Pt 5$d$-Co 3$d$ hybridization across the interface. An application of the MCXD sum rules [10] shows that the $N$-edge MCXD is opposite in sign to the $M$- and $O$-edge MCXD and that the $m_{\mathrm{orb}}$ contribution to a MCXD asymmetry is smaller in the $N_{6,7}$ edges than in the $O_{2,3}$ edges. Thus, the present results provide clear evidence that the induced total Pt moment has a substantial Pt $m_{\mathrm{orb}}$ contribution and is aligned parallel to the total Co moment.

The most interesting feature in Fig. 1 is that the MCXD signals at the Pt $N_{6,7}$ and $O_{2,3}$ edges persist for $t_{\mathrm{Co}}$ down to the thinnest limit. If the Co 3$d$-Pt 5$d$ hybridization extended far into the inside of Co layers, the Pt-edge MCXD arising from the 3$d$-5$d$ hybridization should

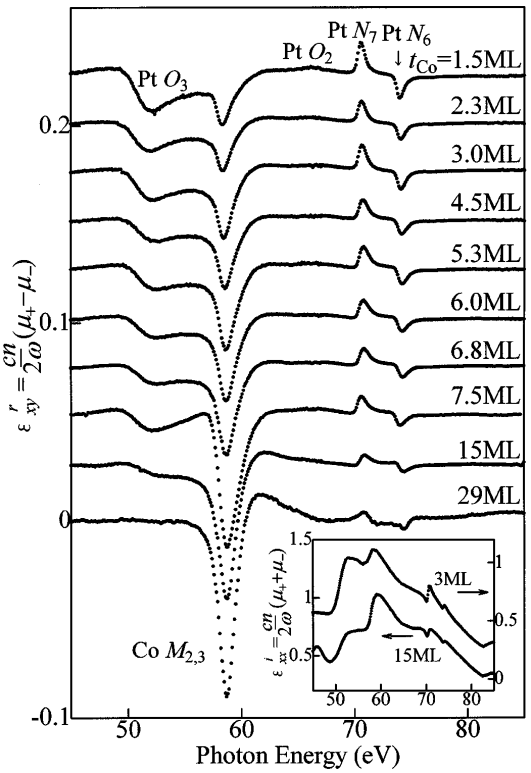


FIG. 1. Absorption MCXD spectra of Co($t_{\mathrm{Co}}$)/Pt(7.5 ML) multilayers around the Co $M_{2,3}$ and Pt $N_{6,7}$ and $O_{2,3}$ edges deduced from reflection MCXD and reflectivity spectra by the Kramers-Kronig analysis. Correction for $P_{\mathrm{C}}$ was made. The inset shows normal absorption for $t_{\mathrm{Co}} = 3$ and 15 ML.

decrease with decreasing $t_{\mathrm{Co}}$. Therefore, we are led to the conclusion that the Co 3$d$-Pt 5$d$ hybridization is highly localized at the Co/Pt interface. The strong hybridization will push down the interfacial Pt 5$d$ bands of spin parallel to the Co majority spin with respect to the 5$d$ bands of opposite spin, thereby producing the Pt spin moment parallel to that of Co. The strong Pt SO coupling could result in a proportionally large $m_{\mathrm{orb}}$ of Pt.

Figure 2(a) shows the flux-normalized polarization-dependent Co $L_{2,3}$ XAS ($\mu_+$ and $\mu_-$) spectra for $t_{\mathrm{Co}} = 3$ and 15 ML. Here, $\mu_+$ and $\mu_-$ stand for the absorption coefficients of the photon helicity parallel and antiparallel to the spin of the Co 3$d$ majority electrons, respectively. The thin solid curve represents the background in XAS [$(\mu_+ + \mu_-)/2$] simulated by a two-step function. Figure 2(b) displays the MCXD spectra normalized by an edge jump in XAS above ~820 eV, providing the MCXD of a per-atom basis. A correction for $P_{\mathrm{C}}$ was made using a calculated average value of 95%. The MCXD orbital sum rule [10] allows us to determine $m_{\mathrm{orb}}$ from the MCXD and XAS spectra by the equation

$$m_{\mathrm{orb}} = -\frac{4\int_{L_3+L_2}(\mu_+ - \mu_-)\,d\omega}{3\int_{L_3+L_2}(\mu_+ + \mu_-)\,d\omega}(10 - n_{3d}), \quad (1)$$

where $m_{\mathrm{orb}}$ is in units of $\mu_{\mathrm{B}}$/atom and $n_{3d}$ is the 3$d$

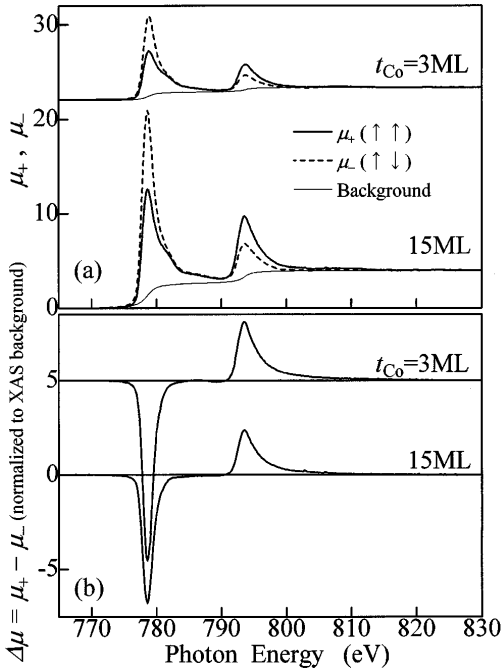


FIG. 2. (a) Polarization-dependent Co $L_{2,3}$ XAS spectra of Co($t_{Co}$)/Pt(7.5 ML) multilayers for $t_{Co} = 3$ and 15 ML. Correction for $P_C$ was made. The thin solid curve denotes the averaged XAS background. (b) Co $L_{2,3}$ MCXD spectra normalized by the edge jump above 820 eV in XAS of (a).

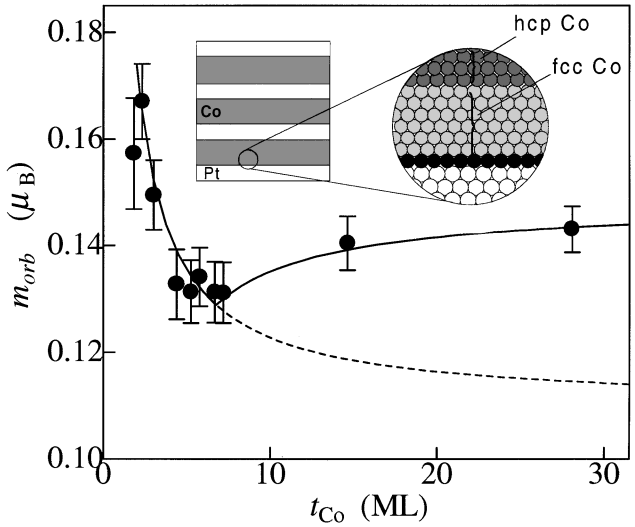


FIG. 3. Orbital magnetic moment of Co perpendicular to the film plane as determined from the MCXD and XAS spectra of Fig. 2 using the MCXD orbital sum rule. The solid curve represents a fit to the data based on the model shown in the inset. The dashed curve denotes an extrapolation for a supposed case of all fcc Co layers.

electron occupation number. We use $n_{3d} = 7.55$ for $t_{Co} \leq 8$ ML from a reported calculation for a $Co_2Pt_4(111)$ multilayer and $n_{3d} = 7.51$ for $t_{Co} \geq 15$ ML as averaged from calculated values for bulk Co [19,20].

Figure 3 shows $m_{orb}$ of Co as a function of $t_{Co}$, as determined from integrating the MCXD and background-subtracted XAS spectra using Eq. (1). It is most noted that $m_{orb}$ increases rapidly with decreasing $t_{Co}$ below $t_{Co} = 6-8$ ML. The $m_{orb}$ enhancement just corresponds to the appearance of PMA confirmed by the present torque magnetometry. Another interesting feature to note is a gradual increase of $m_{orb}$, but not a monotonic decrease with increasing $t_{Co}$ above $t_{Co} = 6-8$ ML. This nonmonotonic behavior is in sharp contrast to the monotonic $m_{orb}$ decrease with increasing $t_{Co}$ observed in an Au/Co/Au(111) staircase [13] and Co films on Cu(100) [21]. The dependence of the present Kerr rotation angle on $t_{Co}$ exhibited a clear kink at $t_{Co} = 6-8$ ML. This indicates a structural transition from fcc to hcp Co at $t_{Co} = 6-8$ ML, where added Co layers start to take the hcp structure with increasing $t_{Co}$ [22]. The abnormal behavior in Fig. 3 corresponds nicely to this observation. We thus attribute the rapid $m_{orb}$ increase for $t_{Co} < 6-8$ ML, except for $t_{Co} = 1.5$ ML, to an enhancement of $m_{orb}$ of Co in the interfacial region and the gradual $m_{orb}$ increase for $t_{Co} > 6-8$ ML to the $m_{orb}$ contribution of hcp Co. The $t_{Co} = 1.5$ ML sample should be accurately represented as $Co_{38}Pt_{62}$-alloy layers separated by Pt layers if an interdiffusion is considered. This could cause a reduced Curie temperature for the film as compared with the others, resulting in an observed $m_{orb}$ for $t_{Co} = 1.5$ ML lower than that for $t_{Co} = 2.3$ ML.

The samples with $t_{Co} \geq 2.3$ ML could essentially retain the interfacial nature despite an intermixing, in the sense that the probability for Co atoms to have adjacent Pt atoms in the perpendicular direction is much higher than having neighboring in-plane Pt atoms. Thus, we consider the simplest model shown in the inset of Fig. 3, by assuming that the $m_{orb}$ enhancement is localized only in a single atomic interface layer. A fit to the data has been made for $t_{Co} \geq 2$ ML by taking $m_{orb}$ of bulk fcc Co ($m_{orb}^{fcc}$), that of bulk hcp Co ($m_{orb}^{hcp}$), and the excessive $m_{orb}$ of a single interface Co layer ($\Delta m_{orb}$) as parameters. The result is shown by the solid curve in Fig. 3. The dashed curve denotes a supposed extrapolation for all of the fcc Co layers, being in clear disagreement with the experimental points. The fitting yields $m_{orb}^{fcc} = (0.110 \pm 0.01)\mu_B$/atom, $m_{orb}^{hcp} = (0.148 \pm 0.005)\mu_B$/atom, and $\Delta m_{orb} = (0.064 \pm 0.01)\mu_B$/atom. The present value of $m_{orb}^{hcp}$ agrees excellently with the results of the gyromagnetic ratio [23] and MCXD [24] measurements, and also with an orbital-polarization local-spin-density approximation (OP-LSDA) calculation [15]. This ensures our analytical procedure. Several calculations [15,25] have been reported on $m_{orb}^{fcc}$; some of them give $m_{orb}^{fcc}$ values that are smaller than $m_{orb}^{hcp}$, while others yield the same value for them. Tischer *et al.* [21] reported a ratio of $m_{orb}^{fcc}/m_{spin}^{fcc}$, but not $m_{orb}^{fcc}$, itself, for fcc Co/Cu(100) from MCXD measurements. Our result is the first experimental determination of $m_{orb}^{fcc}$, and verifies the OP-LSDA calculation [15]. The good agreement between the data and the fitting based on the model leads us to conclude again that the enhancement of perpendicular Co $m_{orb}$ is

localized at the interface, being consistent with the results of the Pt $N_{6,7}$ and $O_{2,3}$ MCXD. The above analysis yields a perpendicular moment of $m_{\rm orb} = 0.174\mu_{\rm B}$/atom for a single Co interface layer. By using Bruno's expression [7] and assuming the in-plane moment being the same as that of bulk fcc Co, we obtain a magnetic anisotropy energy of $\Delta E_{SO} \simeq -(2.3-1.0) \times 10^{-4}$ eV/atom for $t_{\rm Co} = 2-5$ ML, which is larger than the spin-spin dipole interaction energy of $2\pi M_s^2 \simeq +0.92 \times 10^{-4}$ eV/atom and thus drives PMA. The $m_{\rm orb}^{\rm fcc}$ value smaller than the $m_{\rm orb}^{\rm hcp}$ value promotes the tendency to PMA. If the interface in-plane moment is smaller than that of bulk fcc Co [13], $|\Delta E_{\rm SO}|$ should be larger than that estimated above, favoring PMA.

Since most of the Co $3d$ majority-spin bands are located below the Fermi energy ($E_F$), we consider only the Co minority-spin bands. The $z$ axis is taken normally to the film plane and the $x$ axis is chosen to be the in-plane spin quantization axis. The interface hybridization can be viewed as an effective uniaxial crystal field acting on the interface Co atoms. The orbital moment and the resultant magnetic anisotropy originate from the SO interaction given by the Hamiltonian $H_{\rm SO} = \xi_{3d}\boldsymbol{l} \cdot \boldsymbol{s}$ with $\xi_{3d}$ being the SO coupling constant of Co. The matrix elements with the same spin $\langle d_{xy}|H_{\rm SO}|d_{x^2-y^2}\rangle$ and $\langle d_{xz}|H_{\rm SO}|d_{yz}\rangle$ will produce the perpendicular $m_{\rm orb}$ which drives PMA [7]. First, we note that the absolute value of $\langle d_{xy}|H_{\rm SO}|d_{x^2-y^2}\rangle$ is the largest among nonzero matrix elements. Thus, when the crystal field locates the $d_{xy}$ and $d_{x^2-y^2}$ states near to $E_F$ with one being below $E_F$ and the other above $E_F$ with an energy separation smaller than in bulk Co, the perpendicular $m_{\rm orb}$ will be strongly enhanced. Second, the $d_{yz}$ and $d_{xz}$ states, which are degenerate at high-symmetry points in the Brillouin zone, will be split by $H_{\rm SO}$ into two states having orbital moments $\pm\mu_{\rm B}$ of zeroth-order of $\xi_{3d}$ with an energy separation of $\xi_{3d}$ ($\simeq 70$ meV). The ratio of their occupation probability is $\exp(-\xi_{3d}/k_{\rm B}T) \simeq 0.07$ at room temperature. Hence, if the crystal field happens to locate the $d_{yz,xz}$ states within $\sim \xi_{3d}/2$ of $E_F$, just as in a theoretical prediction for the $\bar{M}$ point in Co/Pd multilayers [4], this will result in a large perpendicular $m_{\rm orb}$. These two situations could occur only for a special crystal-field strength and an appropriate position of $E_F$, which could explain why PMA appears only for a limited combination of metals and a particular crystal orientation.

Several theoretical studies [3,4] predicted that the large SO coupling of Pd plays an important role in producing PMA in Co/Pd multilayers. Since the SO interaction of Pt is stronger than that of Pd, it is highly likely that the observed $m_{\rm orb}$ of Pt could contribute appreciably to PMA in Co/Pt multilayers.

Now we have a clear picture of PMA in which the strong interfacial $d$-$d$ hybridization produces an enhanced perpendicular Co $m_{\rm orb}$, which causes PMA by the SO coupling, being further favored by $m_{\rm orb}^{\rm fcc}$ smaller than $m_{\rm orb}^{\rm hcp}$ and by a substantial Pt $m_{\rm orb}$ in Co/Pt multilayers.

The authors thank Professor H. Sugawara, at High Energy Accelerator Research Organization, and Professor H. Kobayakawa for financial support and encouragement.

[1] U. Gradmann and J. Müller, Phys. Status Solidi **27**, 313 (1968); P. F. Carcia *et al.*, Appl. Phys. Lett. **47**, 178 (1985).
[2] P. F. Carcia, J. Appl. Phys. **63**, 5066 (1988); B. N. Engel *et al.*, Phys. Rev. Lett. **67**, 1910 (1991); F. J. A. den Broeder *et al.*, J. Magn. Magn. Mater. **93**, 562 (1991).
[3] J. G. Gay and R. Richter, Phys. Rev. Lett. **56**, 2728 (1986); G. H. O. Daalderop *et al.*, *ibid.* **68**, 682 (1992); Phys. Rev. B **42**, 7270 (1990); *ibid.* **50**, 9989 (1994).
[4] D.-S. Wang *et al.*, Phys. Rev. Lett. **70**, 869 (1993); Phys. Rev. B **48**, 15 886 (1993); J. Magn. Magn. Mater. **129**, 237 (1994); R. Wu *et al.*, *ibid.* **99**, 71 (1991).
[5] B. N. Engel *et al.*, Phys. Rev. B **48**, 9894 (1993); P. Beauvillain *et al.*, J. Appl. Phys. **76**, 6078 (1994).
[6] B. Újfalussy *et al.*, Phys. Rev. Lett. **77**, 1805 (1996); L. Zhong *et al.*, Phys. Rev. B **53**, 9770 (1996).
[7] P. Bruno, Phys. Rev. B **39**, 865 (1989); in *Physical Origins and Theoretical Models of Magnetic Anisotropy* (Ferienkurse des Forschungszentrums Jülich, Jülich, 1993).
[8] G. Schütz *et al.*, Phys. Rev. Lett. **58**, 737 (1987).
[9] C. T. Chen *et al.*, Phys. Rev. B **42**, 7262 (1990); T. Koide *et al.*, *ibid.* **44**, 4697 (1991).
[10] B. T. Thole *et al.*, Phys. Rev. Lett. **68**, 1943 (1992); P. Carra *et al.*, *ibid.* **70**, 694 (1993); J. Stöhr and H. König, *ibid.* **75**, 3748 (1995).
[11] Y. Wu *et al.*, Phys. Rev. Lett. **69**, 2307 (1992); D. Weller *et al.*, Phys. Rev. B **49**, 12 888 (1994).
[12] T. Koide *et al.*, Phys. Rev. B **53**, 8219 (1996); N. Nakajima *et al.*, J. Electron Spectrosc. Relat. Phenom. **78**, 271 (1996).
[13] D. Weller *et al.*, Phys. Rev. Lett. **75**, 3752 (1995).
[14] G. Schütz *et al.*, J. Appl. Phys. **67**, 4456 (1990); J. Vogel *et al.*, Phys. Rev. B **55**, 3663 (1997).
[15] O. Eriksson *et al.*, Phys. Rev. B **42**, 2707 (1990).
[16] Y. Kagoshima *et al.*, Rev. Sci. Instrum. **63**, 1289 (1992); *ibid.* **66**, 1696 (1995).
[17] T. Koide *et al.*, Rev. Sci. Instrum. **63**, 1462 (1992).
[18] T. Koide *et al.*, Nucl. Instrum. Methods Phys. Res., Sect. A **336**, 368 (1993).
[19] R. Wu and A. J. Freeman, Phys. Rev. Lett. **73**, 1994 (1994); G. Y. Guo *et al.*, Phys. Rev. B **50**, 3861 (1994).
[20] An analytical procedure to avoid using theoretical $n_{3d}$ values was employed in Refs. [11] and [13]. However, the procedure, what they call transferrability, is based on successive steps of several assumptions as well as on the use of theoretical values for the Co moments. We do not adopt the method for this reason.
[21] M. Tischer *et al.*, Phys. Rev. Lett. **75**, 1602 (1995).
[22] D. Weller *et al.*, J. Phys. Chem. Solids **56**, 1563 (1995).
[23] D. Bonnenberg *et al.*, in *Magnetic Properties of 3d, 4d, and 5d Elements, Alloys and Compounds*, edited by K.-H. Hellwege and O. Madelung, Landolt-Börnstein (Springer-Verlag, Berlin, 1986), Vol. III/19a, p. 178.
[24] C. T. Chen *et al.*, Phys. Rev. Lett. **75**, 152 (1995).
[25] J. Igarashi and K. Hirai, Phys. Rev. B **53**, 6442 (1996).